Measurements of PL spectra, lifetime and quantum yield

PL spectra were recorded on an Edinburgh Instruments (EI) FLS1000 spectrofluorometer equipped with a continuous (450 W) xenon lamp. The excitation wavelength is 365 nm.

PL decay curves were recorded on a fluorescent lifetime spectrometer (FLS1000) based on a time correlated single photon counting technique under the excitation of 375 nm picosecond laser.

PLQY is defined as the ratio of the emitted photons to the absorbed photons, and was measured by a spectrofluoremeter (FLS1000). An integrating sphere was mounted on the spectrofluoremeter with the entrance and exit ports located in 90^{o} geometry. The PiG sample was located in the center of the integrating sphere. All the recorded spectroscopic data were corrected for the spectral responses of both the spectrofluoremeter and the integrating sphere. The responses of the detecting systems (integrating sphere, monochromators and detectors) in photon flux were determined using a calibrated tungsten lamp. Based on this setup, PLQY is calculated by the following equitation:

$$\eta = \frac{number\ of\ \ photons\ emitted}{number\ of\ \ photons\ absorbed} = \frac{L_{sample}}{E_{reference} - E_{sample}}$$

where η represents QY, L_{sample} the emission intensity, $E_{reference}$ and E_{sample} the intensities of the excitation light not absorbed by the reference and the sample respectively. The precursor glass was used as the standard reference. The difference in integrated areas between the sample and the reference represents the number of the absorbed photons. The photons emitted were determined by integrating the area of the emission band.

Figure S1. Fluorescence image of 9-AA powder (under 365nm UV-light).

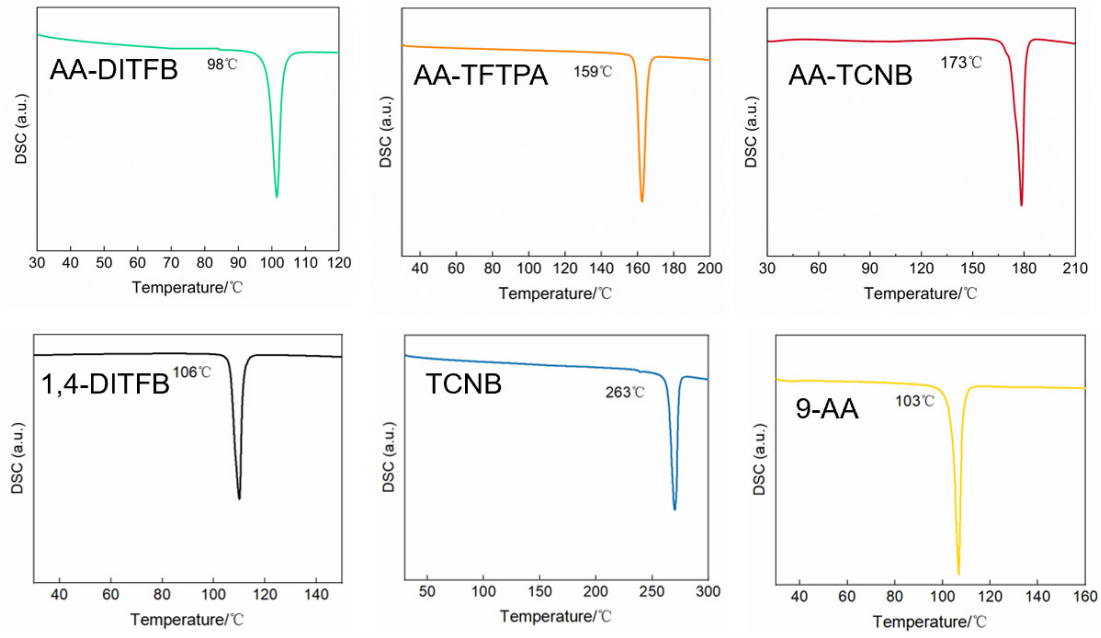

Figure S2. DSC of single components and cocrystals.

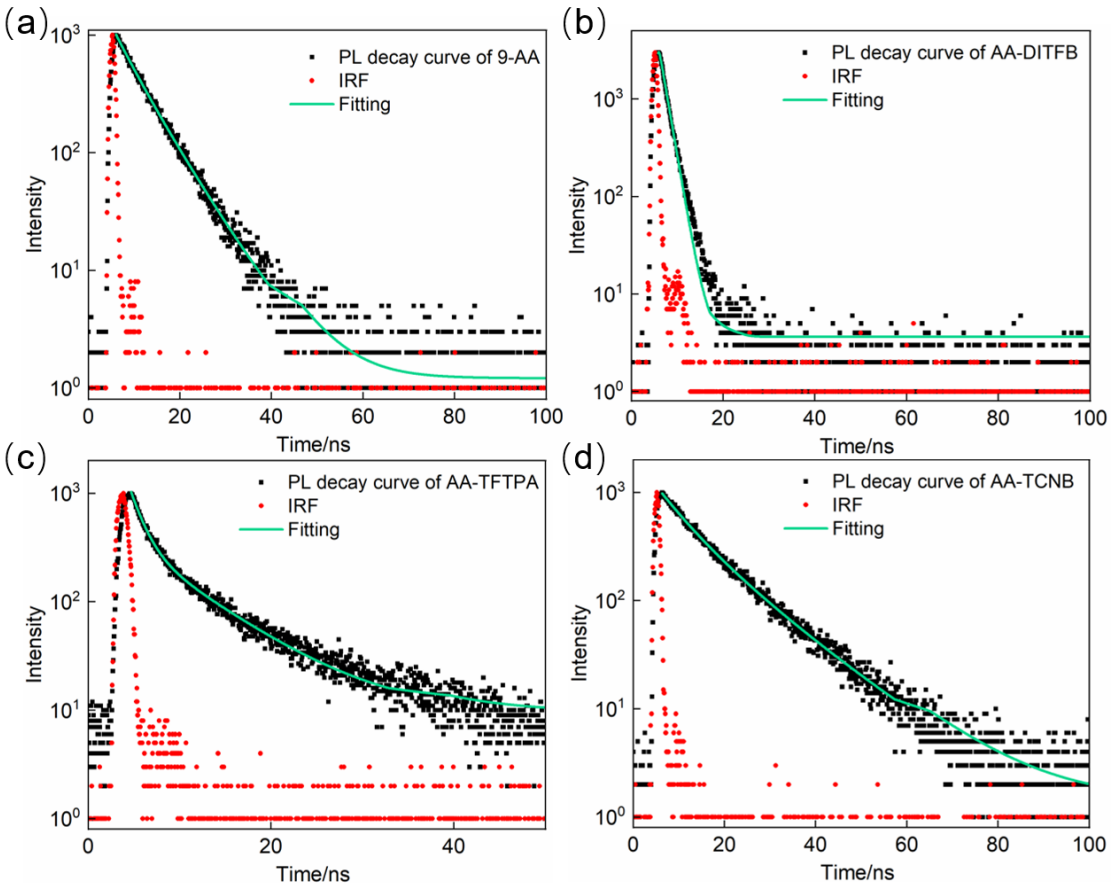

Figure S3. PL decay curves of (a) 9-AA, (b) AA-DITFB, (c) AA-TFTPA and (d) AA-TCNB.

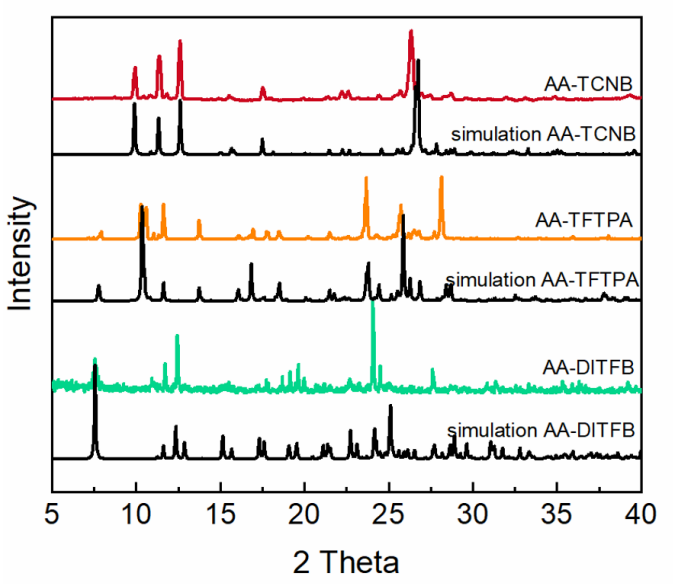

Figure S4. Comparison of experimentally measured PXRD and single crystal simulated PXRD.

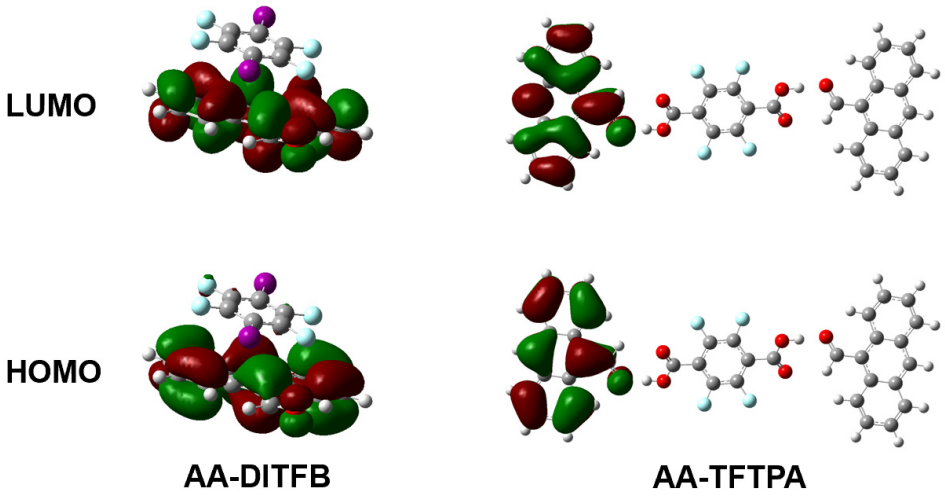

Figure S5. Molecular orbitals of AA-DITFB and AA-TFTPA.

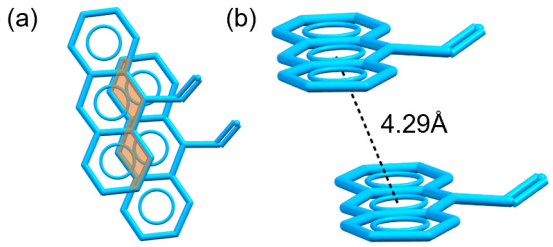

Figure S6. (a) The degree of overlap and (b) the distance between the centroids of adjacent 9-AA molecules in 9-AA crystals.

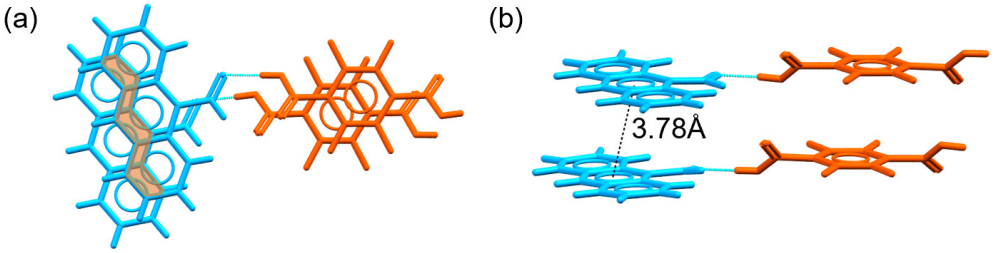

Figure S7. (a) The degree of overlap and (b) the distance between the centroids of adjacent 9-AA molecules in AA-TFTPA crystals.

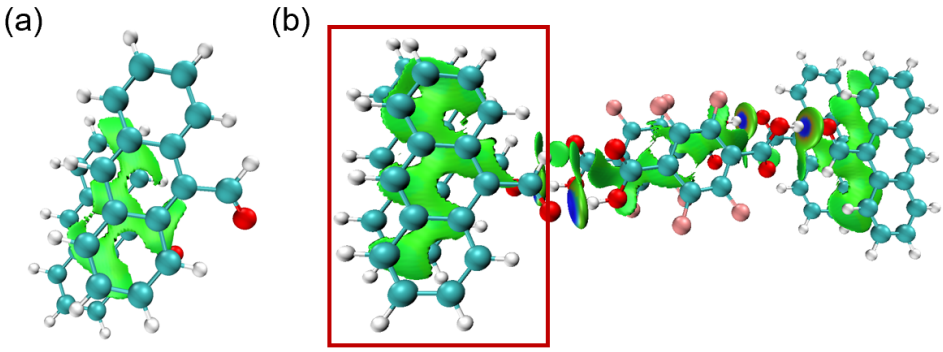

Figure S8. IGMH analysis of (a) 9-AA and (b) AA-TFTPA.

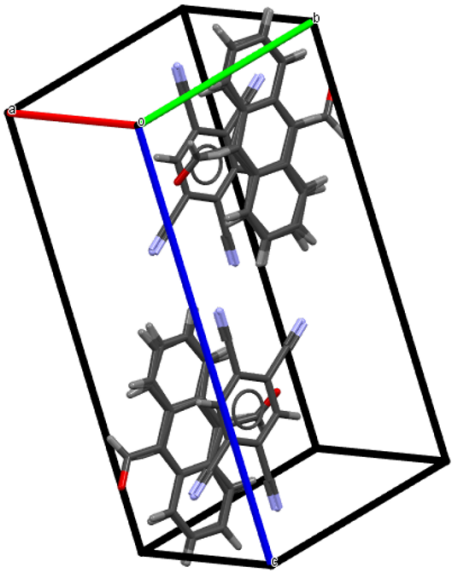

Figure S9. Unit cell of AA-TCNB.

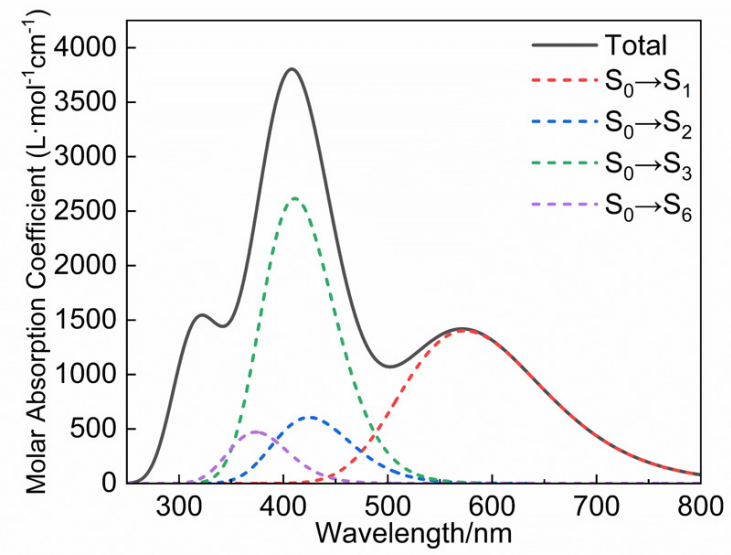

Figure S10. Absorption spectra of AA-TCNB calculated by TDDFT.

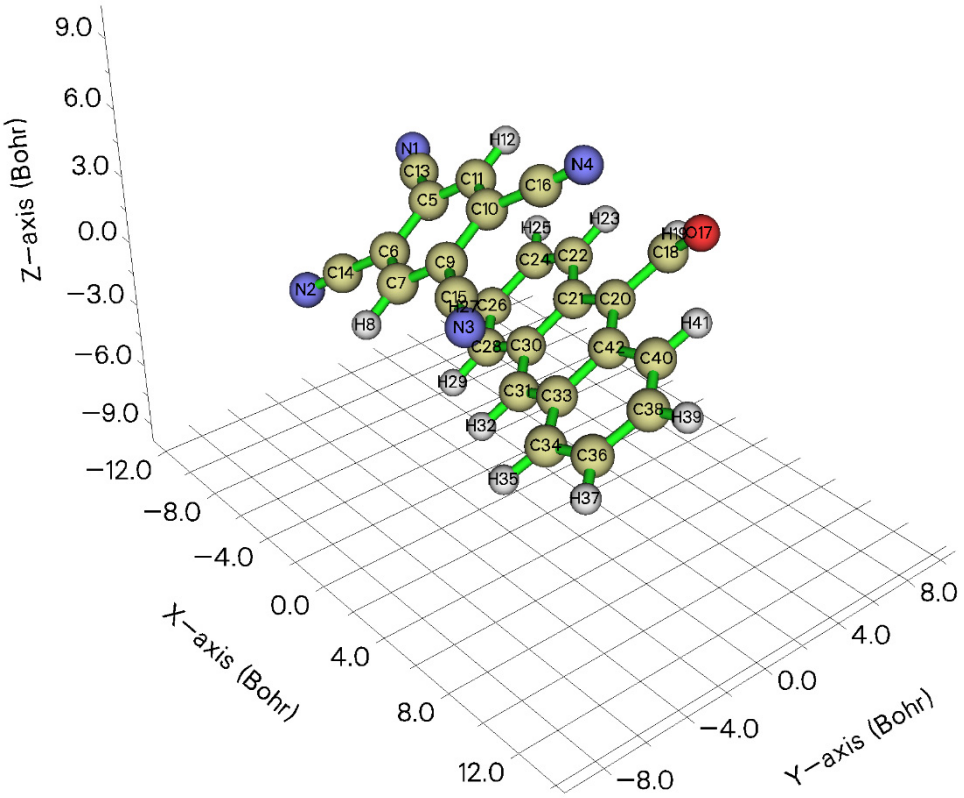

Figure S11. Cartesian coordinates of the optimized geometries of AA-TCNB.

Table S1. Crystallographic data of AA-DITFB, AA-TFTPA and AA-TCNB

Compound	**AA-DITFB**	**AA-TFTPA**	**AA-TCNB**
empirical formula	$C_{21}H_{10}F_4I_2O$	$C_{38}H_{22}F_4O_6$	$C_{25}H_{12}N_4O$
formula weight	608.09	650.55	384.39
temperature (K)	113.15	113.15	113.15
radiation	0.71073	0.71073	0.71073
crystal system	monoclinic	monoclinic	triclinic
space group	$P2_1/n$	$P2_1/c$	P_1
a (Å)	7.8562(2)	10.8144(4)	6.7855(5)
b (Å)	16.9242(3)	12.4283(5)	8.1332(7)
c (Å)	14.8075(4)	21.9174(7)	17.3701(16)
α (°)	90	90	96.489(7)
β (°)	103.962(3)	97.987(3)	94.769(7)
γ (°)	90	90	103.283(7)
V(Å^3)	1910.64(8)	2917.22(19)	921.08(14)
Z	4	4	2
ρ_{calc} (g/cm^3)	2.114	1.481	1.386
F (000)	1144	1336	396
reflections collected	23381(R_{int}=0.0403)	43318(R_{int}=0.0540)	3453(R_{int}=0.0540)
goodness of fit indicator	1.105	1.049	1.080
R_1/wR_2 [$I > 2\sigma(I)$]	0.0271/0.0634	0.0585/0.1436	0.0998/0.2357
R_1/wR_2 [all reflections]	0.0317/0.0654	0.0869/0.1624	0.1333/0.2532
Maximum peak in Final Diff. Map (Å^3)	0.765e$^-$	0.567e$^-$	0.398e$^-$
Minimum peak in Final Diff. Map (Å^3)	− 0.641e$^-$	− 0.274e$^-$	− 0.442e$^-$
Deposition Number	2246517	2246518	2246516

Table S2. Major orbital transition contributions in excited states of AA-TCNB

State	Orbital transition	Contribution	E_{VA}/eV	f	λ/nm
S_1	HOMO→LUMO	99.4%	2.16	0.0312	574
S_2	HOMO→LUMO+2	97.4%	2.9204	0.0135	424
S_3	HOMO→LUMO+1	88.2%	3.0172	0.0582	411
S_4	HOMO-1→LUMO HOMO-1→LUMO+1 HOMO→LUMO+1	68.6% 18.6% 7.1%	3.1377	0.0081	395
S_5	HOMO-1→LUMO+1 HOMO-1→LUMO	59.4% 24.4%	3.2214	0.0011	385
S_6	HOMO-2→LUMO	94.1%	3.3179	0.0105	374
S_7	HOMO-3→LUMO	95.7%	3.6937	0.0039	336
S_8	HOMO-2→LUMO+1 HOMO→LUMO+3	62.0% 27.1%	3.8211	0.0194	324
S_9	HOMO-1→LUMO+2	95.2%	3.9676	0.0048	312
S_{10}	HOMO-2→LUMO+2	97.4%	4.1153	0.0101	301